Monthly Notices of the ROYAL ASTRONOMICAL SOCIETY

MNRAS **461,** L32–L36 (2016) doi:10.1093/mnrasl/slw091
Advance Access publication 2016 May 11

A stellar feedback origin for neutral hydrogen in high-redshift quasar-mass haloes

Claude-André Faucher-Giguère,[1⋆] Robert Feldmann,[2] Eliot Quataert,[2] Dušan Kereš,[3] Philip F. Hopkins[4] and Norman Murray[5†]

[1]*Department of Physics and Astronomy and Center for Interdisciplinary Exploration and Research in Astrophysics (CIERA), Northwestern University, 2145 Sheridan Road, Evanston, IL 60208, USA*
[2]*Department of Astronomy and Theoretical Astrophysics Center, University of California, Berkeley, CA 94720-3411, USA*
[3]*Department of Physics, Center for Astrophysics and Space Sciences, University of California, San Diego, 9500 Gilman Drive, La Jolla, CA 92093, USA*
[4]*TAPIR, Mailcode 350-17, California Institute of Technology, Pasadena, CA 91125, USA*
[5]*Canadian Institute for Theoretical Astrophysics, 60 St. George Street, University of Toronto, ON M5S 3H8, Canada*

Accepted 2016 May 6. Received 2016 May 5; in original form 2016 January 26

ABSTRACT

Observations reveal that quasar host haloes at $z \sim 2$ have large covering fractions of cool dense gas ($\gtrsim$60 per cent for Lyman limit systems within a projected virial radius). Most simulations have so far failed to explain these large observed covering fractions. We analyse a new set of 15 simulated massive haloes with explicit stellar feedback from the FIRE project, covering the halo mass range $M_{\rm h} \approx 2 \times 10^{12} - 10^{13}\,{\rm M}_{\odot}$ at $z = 2$. This extends our previous analysis of the circum-galactic medium of high-redshift galaxies to more massive haloes. Active galactic nuclei (AGN) feedback is not included in these simulations. We find Lyman limit system covering fractions consistent with those observed around quasars. The large H I covering fractions arise from star formation-driven galactic winds, including winds from low-mass satellite galaxies that interact with cosmological filaments. We show that it is necessary to resolve these satellite galaxies and their winds to reproduce the large Lyman limit system covering fractions observed in quasar-mass haloes. Our simulations predict that galaxies occupying dark matter haloes of mass similar to quasars but without a luminous AGN should have Lyman limit system covering fractions comparable to quasars.

Key words: galaxies: evolution – galaxies: formation – galaxies: haloes – intergalactic medium – quasars: absorption lines – cosmology: theory.

1 INTRODUCTION

Spectroscopic measurements of gas flows around galaxies using sight lines to background quasars provide one of the most direct ways of probing the cosmological inflows and galactic outflows that regulate galaxy growth. Over the past several years, this technique has been used at both low redshift and around the peak of the cosmic star formation history at $z \gtrsim 2$ (e.g. Adelberger et al. 2003; Hennawi et al. 2006; Steidel et al. 2010; Tumlinson et al. 2011; Turner et al. 2014). The technique has also been applied to a wide range of foreground objects, including dwarf galaxies (e.g. Bordoloi et al. 2014), damped Lyα absorbers (e.g. Rubin et al. 2015), luminous red galaxies (e.g. Gauthier, Chen & Tinker 2010), $\sim L^{\star}$ star-forming galaxies (e.g. Rudie et al. 2012), and quasars (e.g. Prochaska, Hennawi & Simcoe 2013). Driven by this explosion in high-quality observations, many groups have used cosmological simulations to make predictions for circum-galactic medium (CGM) absorbers (e.g. Faucher-Giguère & Kereš 2011; Kimm et al. 2011; Fumagalli et al. 2011; Goerdt et al. 2012; Stinson et al. 2012; Shen et al. 2013; Hummels et al. 2013; Suresh et al. 2015). Such comparisons are particularly valuable as state-of-the-art cosmological galaxy formation models have now broadly converged on their predictions for the global stellar properties of galaxy populations but diverge strongly on their predictions for gas properties (Somerville & Davé 2015). Thus, CGM observations can break degeneracies between galaxy formation theories.

Our focus in this Letter is on the CGM of galaxies likely to be traced by luminous quasars at $z \sim 2$, which have a characteristic halo mass $M_{\rm h} \sim 10^{12.5}\,{\rm M}_{\odot}$ (e.g. White et al. 2012). Prochaska et al. (2013, hereafter PHS13) reported a surprisingly high covering fraction $f_{\rm cov}(>10^{17.2};\ <R_{\rm vir}) \approx 0.64^{+0.06}_{-0.07}$ of Lyman limit systems (LLSs; $N_{\rm H\,I} > 10^{17.2}\ {\rm cm}^{-2}$) within a projected virial radius of $z \sim 2-2.5$ quasars (see also Prochaska, Lau & Hennawi 2014). The high covering fraction of cool gas in quasar haloes is in contrast to the lower fraction $f_{\rm cov}(10^{17.2};\ <R_{\rm vir}) = 0.30 \pm 0.14$ measured by Rudie et al. (2012) around $z \sim 2 - 2.5$ Lyman break galaxies (LBGs) in the Keck Baryonic Structure Survey (KBSS). The LBGs in KBSS reside in dark matter haloes of characteristic mass $M_{\rm h} \approx 10^{12}\,{\rm M}_{\odot}$

⋆ E-mail: cgiguere@northwestern.edu
† Canada Research Chair in Astrophysics.

(Adelberger et al. 2005), a factor ∼3 lower than luminous quasars. Using cosmological zoom-in simulations of galaxy formation with stellar feedback but neglecting the effects of active galactic nuclei (AGN), Fumagalli et al. (2014) and Faucher-Giguère et al. (2015, hereafter FG15) showed that the LLS covering fractions in the simulations were broadly consistent with those measured in LBG haloes (see also Shen et al. 2013). Both studies however concluded that the most massive haloes in their analyses could not explain the LLS covering fractions measured around quasars (but see Schaye et al. 2015, which we discuss further in Section 3.1).

In this Letter, we extend the FG15 analysis with a new set of 15 haloes simulated to $z = 2$ with stellar feedback physics from the FIRE ('Feedback In Realistic Environments') project and with masses representative of quasar hosts.[1] These simulations are part of the MassiveFIRE simulation suite described in Feldmann et al. (2016). We use these simulations to revisit the comparison with H I covering fractions measured around $z \sim 2$ quasars. The simulations we analyse here do not include AGN but comparing them observations of quasar-mass haloes is useful because it can show whether the observed covering fractions in quasar haloes require the presence of a luminous AGN or not.

We describe our simulations and analysis methodology in Section 2, discuss our main results in Section 3, and conclude in Section 4. Throughout, we assume a standard ΛCDM cosmology with parameters consistent with the latest constraints ($h \approx 0.7$, $\Omega_m = 1 - \Omega_\Lambda \approx 0.27$ and $\Omega_b \approx 0.046$; Planck Collaboration XIII 2015).

2 SIMULATIONS AND ANALYSIS METHODOLOGY

2.1 Zoom-in simulations

Our simulations implement the same stellar feedback physics and numerical methods as the ones analysed in Hopkins et al. (2014) and FG15; we refer to those papers for details. Briefly, the simulations were run using the GIZMO simulation code in P-SPH mode (Hopkins 2013, 2015). Gas is allowed to cool to $T \sim 10$ K via atomic and molecular lines and star formation proceeds only in dense regions ($n_H > 5\,cm^{-3}$) that are locally self-gravitating. Stellar feedback is modelled by implementing energy, momentum, mass, and metal return from radiation, Supernovae, stellar winds, and photoionization following STARBURST99 (Leitherer et al. 1999). During the course of the hydrodynamical calculation, ionization balance is computed using the ultraviolet background model of Faucher-Giguère et al. (2009) and we apply an on-the-fly correction for self-shielded gas.

Our analysis in this Letter combines the simulations previously analysed in FG15 and new haloes from the MassiveFIRE suite. The MassiveFIRE haloes included in this analysis are the haloes in the mass range $M_h \approx 2 \times 10^{12}$–$10^{13}\,M_\odot$ at $z = 2$ introduced in Feldmann et al. (2016). These haloes span a wide range of accretion histories and environments. A subset of the MassiveFIRE simulations have been run at three resolution levels, labelled LR (low resolution), MR (medium resolution), and HR (high resolution). The HR simulations have a (zoom-in region) gas particle mass $m_b = 3.3 \times 10^4\,M_\odot$ and a minimum (adaptive) gas gravitational softening $\epsilon_b = 9$ proper pc. The dark matter particle mass and gravitational softening lengths in the zoom-in regions are $m_{dm} = 1.7 \times 10^5\,M_\odot$ and $\epsilon_{dm} = 143$ proper pc, respectively. These HR resolution parameters are similar to the 'z2h' simulations and other LBG-mass haloes analysed in FG15. The MR simulations have the same gravitational softening parameters but higher gas and dark matter particle masses by a factor of 8 in zoom-in regions. The LR simulations have higher zoom-in particle masses by another factor of 8, double the minimum gravitational softening lengths of the MR and HR simulations, and a lower star formation density threshold of $n_H = 1\,cm^{-3}$. Our final compilation of covering fractions is based on HR-level simulations only and we focus on $z = 2$–2.5.

In FG15, we concluded that simulations only including stellar feedback failed to explain the large LLS covering fractions observed around $z \sim 2$ quasars. That conclusion was primarily based on our analysis of the m14 simulation ($M_h(z = 2) \approx 6 \times 10^{12}\,M_\odot$). The m14 simulation had a zoom-in gas particle mass $m_b = 4.4 \times 10^6\,M_\odot$ much larger than the HR-level LBG-mass haloes included in the analysis. We show in Section 3.2 that the m14 simulation did not have sufficient resolution to produce converged CGM predictions and so we exclude it from our updated analysis. We also exclude the m13 simulation analysed in FG15 since its resolution was closer to MR level than HR level.

2.2 CGM analysis methodology

Our analysis is similar to that performed in FG15; we only summarize here the key points. To evaluate covering fractions, the particle data are first projected on to a Cartesian grid of side length L centred on the halo with N grid points along each dimension. In this Letter, we focus on LLS covering fractions within a projected virial radius, defined as the fractions of projected pixels with H I column density $N_{HI} > 10^{17.2}\,cm^{-2}$. We use the Bryan & Norman (1998) virial radius definition. For the new massive haloes, we use $L = 600$ proper kpc and $N = 600$, corresponding to a spatial grid resolution of 1 proper kpc. Our LLS covering fractions are well converged with grid resolution. To approximate neutral fractions in self-shielded gas, we use the analytic fits to radiative transfer calculations developed by Rahmati et al. (2013). We neglect ionization of CGM gas by local sources. This tends to overestimate H I covering fractions, but only slightly for LLSs around ordinary galaxies (e.g. Faucher-Giguère & Kereš 2011; Fumagalli et al. 2011). Hennawi & Prochaska (2007) showed that the clustering of LLSs around luminous quasars is highly anisotropic, consistent with LLSs being photo-evaporated along the line of sight but largely unaffected by the quasar radiation in the transverse direction. For our comparison with LLSs transverse to quasars, we thus also neglect local ionization effects.

3 THE CGM OF HIGH-REDSHIFT MASSIVE HALOES

3.1 LLS properties

Fig. 1 shows H I column density, gas-phase metallicity, and stellar surface density maps for three representative high-resolution haloes from the MassiveFIRE sample. The haloes are substantially filled with high-column and metal-enriched H I. The mean, median, and standard deviation of $\log_{10}(Z/Z_\odot)$, where Z is the HI-mass weighted metallicity, for LLS sight lines within a projected R_{vir} (but excluding the inner 20 proper kpc to minimize contamination from the central galaxy) are −1.1, −0.9, and 0.7, respectively (assuming $Z_\odot = 0.14$; Asplund et al. 2009). The projected gas kinematics are complex (velocities up to ∼500 km s^{-1}; see Fig. 1) and it is not generally possible to use LLS metallicity to cleanly separate cosmological inflows or galactic winds in an instantaneous sense (see also Hafen et al., in preparation). Overall, the metallicity and kinematic properties of dense H I in our simulated massive haloes

[1] See project website: http://fire.northwestern.edu

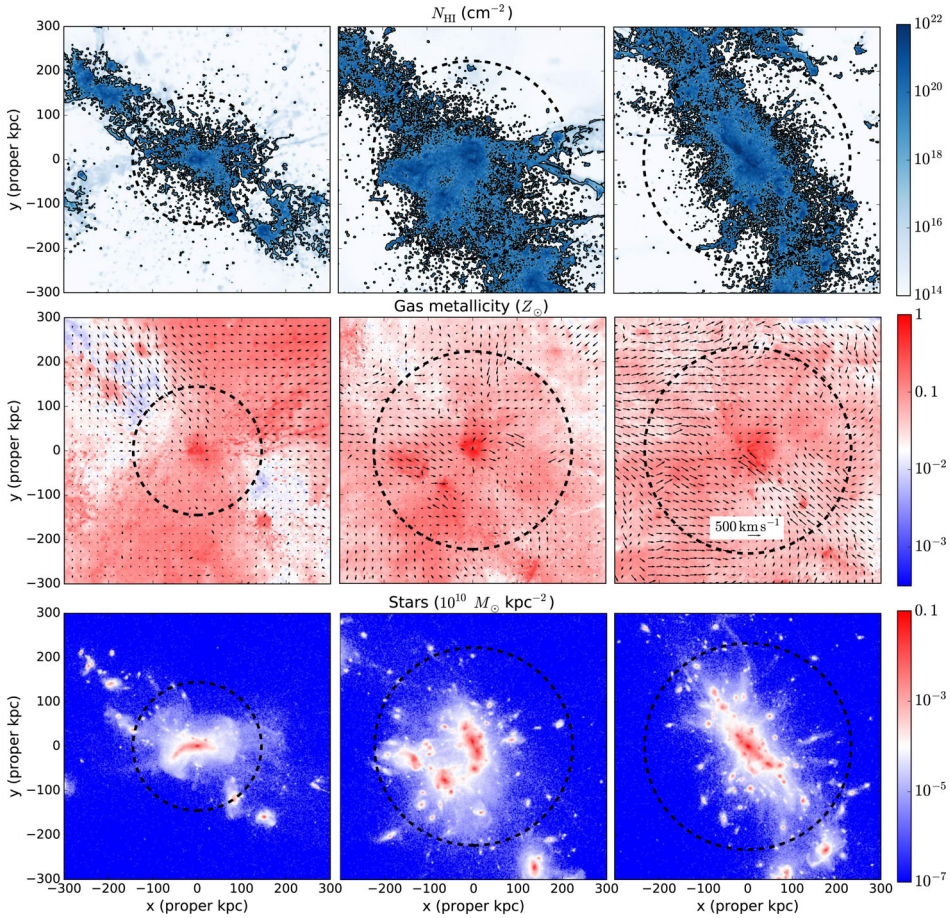

Figure 1. H I column density (top), gas-phase metallicity (middle) and stellar mass surface density (bottom) maps for three representative MassiveFIRE haloes at $z = 2$ (from left to right: $M_{\rm h}(z = 2) = (2.4, 8.8, 9.9) \times 10^{12}\,{\rm M}_\odot$). The virial radius is indicated by dashed circle in each panel and solid contours indicate Lyman limit systems. The vectors on metallicity maps indicate projected mass-weighted velocities.

appear broadly consistent with observational constraints from high-dispersion spectra of the $z \sim 2$ quasar CGM (Lau, Prochaska & Hennawi 2015). Interestingly, the overall spatial distribution of LLSs correlates with the spatial distribution of satellite galaxies, indicating that satellites play an important role in shaping the H I distribution in massive haloes. As we showed for LGB-mass haloes in FG15, ejection of cool gas by both central and satellite galaxies can interact with infalling large-scale structure filaments to enhance LLS covering fractions substantially.

Fig. 2 summarizes the LLS covering fractions evaluated within a projected virial radius for the simulations previously analysed in FG15 and for the new MassiveFIRE haloes at $z = 2$ and $z = 2.5$. The simulated covering fractions are compared to the average covering fractions measured by Rudie et al. (2012) around LBGs and by PHS13 in haloes hosting quasars over matching redshift ranges. To facilitate the comparison of our simulated haloes with the Rudie et al. and Prochaska et al. observational data points, we also show averages over the LBG- and quasar-mass haloes in our simulation sample. The open black circle averages over all haloes of mass $10^{11.5} \leq M_{\rm h} \leq 10^{12.5}\,{\rm M}_\odot$ ($f_{\rm cov} = 0.26 \pm 0.11$) and the open black star averages over all MassiveFIRE haloes ($M_{\rm h} \approx 10^{12} - 10^{13}\,{\rm M}_\odot$; $f_{\rm cov} = 0.55 \pm 0.13$).

Overall, we find good agreement between the simulated and observed covering fractions for both the LBG and quasar samples, with the covering fractions increasing systematically with increasing halo mass and from $z = 2$ to $z = 2.5$. We find much higher covering fractions than in FG15 in our more statistically

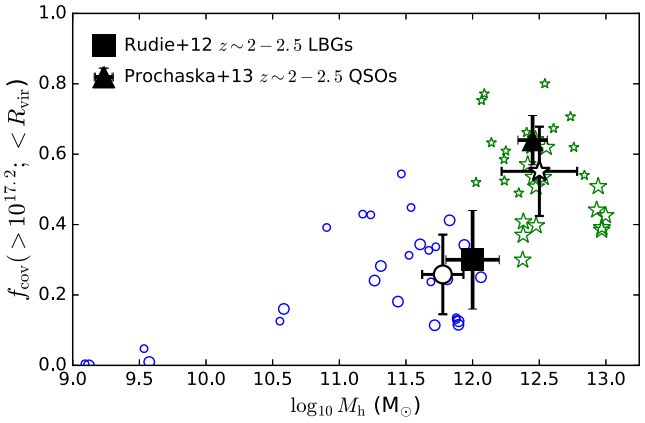

Figure 2. Blue circles: Lyman limit system covering fractions at $z = 2$ (large) and $z = 2.5$ (small) within a projected virial radius for the simulated haloes analysed in FG15 (HR resolution or better only). Green stars: covering fractions at $z = 2$ (large) and $z = 2.5$ (small) for the MassiveFIRE haloes. The open black symbols show averages over simulated LBG-mass haloes and quasar-mass haloes with the error bars showing the standard deviations of the simulated data points included in the averages. We compare the simulated covering fractions to LLS measurements transverse to LBGs at $z \sim 2{-}2.5$ by Rudie et al. (2012) (black square) and transverse to luminous quasars in the same redshift interval by PHS13 (black triangle).

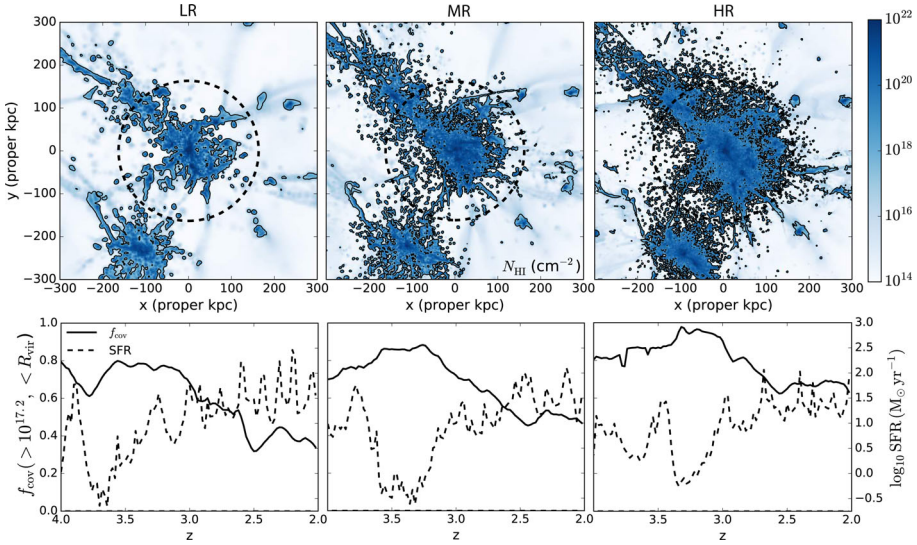

Figure 3. Top: $z = 2$ H I maps for a $M_{\rm h}(z = 2) = 3.6 \times 10^{12}$ M$_\odot$ MassiveFIRE halo simulated at three resolution levels. Bottom: LLS covering fraction and star formation rate within a virial radius from $z = 4$ to $z = 2$. The LLS covering fractions increase systematically with increasing resolution (from left to right), while the burstiness of the star formation history decreases with increasing resolution.

robust and higher-resolution sample of quasar-mass haloes. We explain this difference in the next section. Our predicted covering fractions in quasar-mass haloes are also higher by a factor ∼3 than those predicted by the simulations of Fumagalli et al. (2014). Our simulated haloes include strong stellar feedback but no AGN feedback, suggesting that the high covering fractions measured around quasars do not require a significant contribution from AGN feedback (although such feedback could certainly be important in real haloes).

While the covering fractions appear to increase smoothly from the LBG mass regime to the quasar mass regime, the increase is rather steep: a factor >2 increase in covering fraction for factor of 5 increase in halo mass (computed from the averages shown by the open black symbols in Fig. 2). A few effects likely contribute to this steep increase. First, low-mass main haloes have small H I covering fractions within their virial radii, as can be seen from the open blue symbols in Fig. 2. When such low-mass haloes are the satellites of more massive main haloes, they do not contribute a large LLS cross-section. Quasar-mass haloes, however, can have satellites that are as massive as LBGs and which can each contribute a significant fraction of their virial cross-section as LLSs. In addition, quasar hosting haloes are massive enough that they may be able to sustain a quasi-static hot atmosphere (Birnboim & Dekel 2003; Kereš et al. 2005; Faucher-Giguère, Kereš & Ma 2011) whose pressure may increase the density of cool gas and, more generally, change how cosmological inflows and outflows propagate inside haloes.

In their analysis of the EAGLE simulations, Rahmati et al. (2015) were also able to reconcile the LLS covering fractions predicted by their simulations with those observed around quasars by PHS13. However, the agreement found by Rahmati et al. (2015) is due primarily to a different effect. In their simulations, the median LLS covering fraction within $R_{\rm vir}$ increases by less than 30 per cent from $M_{\rm h} = 10^{12}$ M$_\odot$ to $M_{\rm h} = 10^{13}$ M$_\odot$ at $z = 2$. Instead, Rahmati et al. (2015) find agreement by assuming that all quasars in the PHS13 sample are hosted by haloes with mass $M_{\rm h} > 10^{12.5}$ M$_\odot$ and following the mass distribution of the most massive haloes in the EAGLE box. They then compared PHS13's observations with simulated haloes at fixed transverse proper projection, rather than as a fraction of $R_{\rm vir}$. Since LLS covering fractions decrease with increasing fraction of $R_{\rm vir}$, Rahmati et al. (2015) effectively obtained high covering fractions by assuming that many of PHS13's sight lines probe a smaller fraction of the virial radius of foreground quasars than assumed by PHS13, who reported covering fractions assuming a fixed virial radius appropriate for $M_{\rm h} \approx 10^{12.5}$ M$_\odot$. This highlights the fact that different state-of-the-art feedback models still predict significantly different H I covering fractions around massive high-redshift galaxies.

3.2 Numerical convergence

In Fig. 3, we compare H I maps for HR, MR, and LR runs for a representative $M_{\rm h}(z = 2) = 3.6 \times 10^{12}$ M$_\odot$ halo. The maps show that the LLS covering fractions increase systematically with increasing resolution. This is confirmed more quantitatively by the bottom panels, which show the corresponding covering fractions and star formation rates within the halo for 100 time slices between $z = 4$ and $z = 2$. An important factor determining the high resolution needed to obtain converged H I covering fractions is that it requires not only resolving the generation of galactic winds from central galaxies, but also from lower mass satellites that are represented by a smaller number of resolution elements.

The systematic increase in predicted LLS covering fractions with increased resolution is the most important factor driving the different conclusion that we reached previously (FG15) regarding quasar-mass haloes. That analysis was based primarily on the covering fractions of the m14 simulation. Even the LR version of MF2 has slightly smaller gas particle mass and minimum gas softening length than m14 ($m_{\rm b} = 2.1 \times 10^6$ versus $m_{\rm b} = 4.4 \times 10^6$, and $\epsilon_{\rm b} = 18$ proper pc versus $\epsilon_{\rm b} = 70$ proper pc). The simulated LLS system covering fractions increase slightly even from the SR run to the HR run in Fig. 3, indicating that covering fractions may not be fully converged even in our HR simulations for quasar-mass haloes. We stress, however, that the majority of the LBG-mass haloes analysed in FG15 had resolution similar to the HR runs analysed here and that FG15 demonstrated convergence of their H I covering fractions for those haloes.

Finally, it is worth noting that Fig. 1 shows that the dense H I distribution in our massive haloes is clumpy. In detail, the phase structure of the CGM probably depends not only on the subgrid models for stellar feedback and resolution parameters, but also on

the properties of the hydrodynamic solver employed (e.g. Kereš et al. 2012; Bird et al. 2013) and whether 'non-ideal' hydrodynamical effects such as magnetic forces and thermal conduction are included. Such effects can, for example, significantly affect the survival of cool clouds in galactic winds (e.g. McCourt et al. 2015). It is thus prudent to regard the CGM phase structure (including the detailed temperature distribution of galactic winds) predicted by our simulations as uncertain. Nevertheless, our simulations provide a clear demonstration that an explicit implementation of stellar feedback processes that successfully explains the stellar masses of galaxies without any parameter tuning (Hopkins et al. 2014; Feldmann et al. 2016) also predicts the presence of sufficient cool gas in galaxy haloes to explain LLS covering fractions around both LBGs and quasars at $z \sim 2{-}2.5$.

4 DISCUSSION AND CONCLUSIONS

Our central result is that the MassiveFIRE simulations, with strong stellar feedback but no AGN feedback, predict LLS covering fractions within a projected virial radius in good agreement with those measured by PHS13 around luminous quasars. In our simulations, the covering fractions are high in quasar-mass haloes to large extent because stellar feedback drives galactic winds which interact with and expand cosmological filaments. It is thus critical for simulations to not only resolve the generation of galactic winds from central galaxies but also the winds from satellite galaxies embedded in associated large-scale structure.

Our results suggest that AGN feedback is not necessary to explain the large covering fractions observed around quasars, though it is certainly possible that AGN feedback significantly affects the CGM of real quasars (e.g. Johnson et al. 2015). One way to observationally test whether the presence of a luminous AGN affects the properties of halo gas on $\sim$100 proper kpc scales would be to obtain spectra transverse to foreground galaxies that inhabit haloes of similar mass but do not have a luminous AGN. Such haloes can be traced by highly star-forming sub-millimetre galaxies (e.g. Hickox et al. 2012; Narayanan et al. 2015) or by $z \sim 2$ galaxies selected based on their high stellar mass.

ACKNOWLEDGEMENTS

We grateful for useful discussions with Xavier Prochaska, Joe Hennawi, Ali Rahmati, Zach Hafen, Daniel Anglés-Alcázar, and Alexander Muratov. CAFG was supported by NSF grants AST-1412836 and AST-1517491, by NASA grant NNX15AB22G, and by STScI grants HST-AR-14293.001-A and HST-GO-14268.022-A. RF was supported by NASA through Hubble Fellowship grant HF-51304.01-A. EQ was supported by NASA ATP grant 12-ATP-120183, a Simons Investigator award from the Simons Foundation, and the David and Lucile Packard Foundation. DK was supported by NSF grant AST-1412153. Support for PFH was provided by an Alfred P. Sloan Research Fellowship, NASA ATP grant NNX14AH35G, and NSF grants AST-1411920 and AST-1455342. The simulations analysed in this Letter were run on XSEDE computational resources (allocations TG-AST120025, TG-AST130039, and TG-AST140023) and on NASA High-End Computing resources (allocations SMD-14-5492, SMD-14-5189, and SMD-15-6530).

REFERENCES

Adelberger K. L. et al., 2003, ApJ, 584, 45
Adelberger K. L., Erb D. K., Steidel C. C., Reddy N. A., Pettini M., Shapley A. E., 2005, ApJ, 620, L75
Asplund M., Grevesse N., Sauval A. J., Scott P., 2009, ARA&A, 47, 481
Bird S., Vogelsberger M., Sijacki D., Zaldarriaga M., Springel V., Hernquist L., 2013, MNRAS, 429, 3341
Birnboim Y., Dekel A., 2003, MNRAS, 345, 349
Bordoloi R. et al., 2014, ApJ, 796, 136
Bryan G. L., Norman M. L., 1998, ApJ, 495, 80
Faucher-Giguère C.-A., Kereš D., 2011, MNRAS, 412, L118
Faucher-Giguère C.-A., Lidz A., Zaldarriaga M., Hernquist L., 2009, ApJ, 703, 1416
Faucher-Giguère C.-A., Kereš D., Ma C.-P., 2011, MNRAS, 417, 2982
Faucher-Giguère C. A., Hopkins P. F., Kereš D., Muratov A. L., Quataert E., Murray N., 2015, MNRAS, 449, 987 (FG15)
Feldmann R., Hopkins P. F., Quataert E., Faucher-Giguère C.-A., Kereš D., 2016, MNRAS, 458, L14
Fumagalli M., Prochaska J. X., Kasen D., Dekel A., Ceverino D., Primack J. R., 2011, MNRAS, 418, 1796
Fumagalli M., Hennawi J. F., Prochaska J. X., Kasen D., Dekel A., Ceverino D., Primack J., 2014, ApJ, 780, 74
Gauthier J.-R., Chen H.-W., Tinker J. L., 2010, ApJ, 716, 1263
Goerdt T., Dekel A., Sternberg A., Gnat O., Ceverino D., 2012, MNRAS, 424, 2292
Hennawi J. F., Prochaska J. X., 2007, ApJ, 655, 735
Hennawi J. F. et al., 2006, ApJ, 651, 61
Hickox R. C. et al., 2012, MNRAS, 421, 284
Hopkins P. F., 2013, MNRAS, 428, 2840
Hopkins P. F., 2015, MNRAS, 450, 53
Hopkins P. F. et al., 2014, MNRAS, 445, 581
Hummels C. B., Bryan G. L., Smith B. D., Turk M. J., 2013, MNRAS, 430, 1548
Johnson S. D., Chen H.-W., Mulchaey J. S., 2015, MNRAS, 452, 2553
Kereš D., Katz N., Weinberg D. H., Davé R., 2005, MNRAS, 363, 2
Kereš D., Vogelsberger M., Sijacki D., Springel V., Hernquist L., 2012, MNRAS, 425, 2027
Kimm T., Slyz A., Devriendt J., Pichon C., 2011, MNRAS, 413, L51
Lau M. W., Prochaska J. X., Hennawi J. F., 2015, preprint (arXiv:1510.06018)
Leitherer C. et al., 1999, ApJS, 123, 3
McCourt M., O'Leary R. M., Madigan A.-M., Quataert E., 2015, MNRAS, 449, 2
Narayanan D. et al., 2015, Nature, 525, 496
Planck Collaboration XIII, 2015, preprint (arXiv:1502.01589)
Prochaska J. X., Hennawi J. F., Simcoe R. A., 2013, ApJ, 762, L19 (PHS13)
Prochaska J. X., Lau M. W., Hennawi J. F., 2014, ApJ, 796, 140
Rahmati A., Pawlik A. H., Raicevic M., Schaye J., 2013, MNRAS, 430, 2427
Rahmati A., Schaye J., Bower R. G., Crain R. A., Furlong M., Schaller M., Theuns T., 2015, MNRAS, 452, 2034
Rubin K. H. R., Hennawi J. F., Prochaska J. X., Simcoe R. A., Myers A., Lau M. W., 2015, ApJ, 808, 38
Rudie G. C. et al., 2012, ApJ, 750, 67
Schaye J. et al., 2015, MNRAS, 446, 521
Shen S., Madau P., Guedes J., Mayer L., Prochaska J. X., Wadsley J., 2013, ApJ, 765, 89
Somerville R. S., Davé R., 2015, ARA&A, 53, 51
Steidel C. C., Erb D. K., Shapley A. E., Pettini M., Reddy N., Bogosavljević M., Rudie G. C., Rakic O., 2010, ApJ, 717, 289
Stinson G. S. et al., 2012, MNRAS, 425, 1270
Suresh J., Bird S., Vogelsberger M., Genel S., Torrey P., Sijacki D., Springel V., Hernquist L., 2015, MNRAS, 448, 895
Tumlinson J. et al., 2011, Science, 334, 948
Turner M. L., Schaye J., Steidel C. C., Rudie G. C., Strom A. L., 2014, MNRAS, 445, 794
White M. et al., 2012, MNRAS, 424, 933

This paper has been typeset from a TEX/LATEX file prepared by the author.